S. Afr. J. Chem., 2014, **67**, 27–32,
<http://journals.sabinet.co.za/sajchem/>.

A Simple and Efficient Synthesis of 12-Aryl-8,9,10,12-tetrahydrobenzo[*a*]xanthen-11-ones by ZnO Nanoparticles Catalyzed Three Component Coupling Reaction of Aldehydes, 2-Naphthol and Dimedone

Javad Safaei-Ghomi and Mohammad Ali Ghasemzadeh

Department of Chemistry, Qom Branch, Islamic Azad University, Qom, Iran.

Received 11 September 2013, revised 19 November 2013, accepted 22 January 2014.

ABSTRACT

Highly effective zinc oxide nanoparticles catalyzed solvent-free synthesis of some tetrahydrobenzo[*a*]xanthen-11-one derivatives *via* one-pot multi-component reaction of aldehydes, 2-naphthol and dimedone. The present approach creates a variety of biologically active heterocyclic compounds in excellent yields and short reaction times. Four new compounds are reported. The salient features of the ZnO nanoparticles are: easy preparation, cost-effective, high stability, low loading and reusability of the catalyst. The prepared zinc oxide nanoparticles were fully characterized by EDX, XRD, SEM, IR and TEM analysis.

KEYWORDS

ZnO, nanoparticles, tetrahydrobenzo[*a*]xanthen-11-one, multi-component reactions, heterocyclic compounds.

1. Introduction

Multi-component reactions (MCRs) are special types of synthetically useful organic reactions in which three or more substrates react to give a final product in a one-pot procedure.[1] These reactions are valuable assets in organic synthesis and pharmaceutical chemistry due to their wide range of applications in the preparation of various structural scaffolds and discovery of new drugs.[2]

Xanthene and its derivatives are an important class of oxygen-containing heterocyclic compounds that are known to have important biological and pharmacological activities such as: anti-inflammatory,[3] antibacterial,[4] antiviral[5] and also provide efficacy in photodynamic therapy.[6] In addition, some of the xanthene derivatives can be employed as pH sensitive fluorescent materials,[7] dyes and also in laser technologies.[8,9] Therefore, the synthesis of xanthene derivatives due to a broad range of applications have always been a popular field in organic synthesis.

Among the various xanthene based materials 12-aryl-8,9,10,12-tetrahydrobenzo[*a*]xanthen-11-ones retain a significant place because of their special structure and great potential for developing further synthesis strategies. Three component reactions of aldehydes, 2-naphthol and cyclic 1,3-dicarbonyl compounds is one of the most attractive approaches for the synthesis of 12-aryl-8,9,10,12-tetrahydrobenzo[*a*]xanthen-11-ones. Recently, multi-component synthesis of tetrahydrobenzo[*a*]xanthen-11-ones have been performed in presence of various catalysts such as: sulfamic acid,[10] H_2SO_4,[11] $InCl_3$ or P_2O_5,[12] $[Py(HSO_4)_2]$,[13] cyanuric chloride,[14] iodine,[15] tetradecyltrimethylammoniumbromide (TTAB),[16] biodegradable ionic liquid [DDPA][HSO_4],[17] $HClO_4$-SiO_2.[18]

Some of these procedures have some drawbacks, such as toxic solvents and catalysts, long reaction times, undesirable yields and use of costly catalysts. Thus, it is essential to design an efficient, green and simple method for the preparation of tetrahydrobenzo[*a*]xanthen-11-ones without those disadvantages.

*To whom correspondence should be addressed. E-mail: safaei@kashanu.ac.ir

Recently, nanomaterial-based catalysts as prominent heterogeneous catalysts are widely used in order to accelerate catalytic processes, particularly because they are accompanied with the principle of the green chemistry. Also the separation and recycling of heterogeneous nanoparticles can be easily achieved with more maintenance of catalytic reactivity in comparison to bulk counterparts.[19,20]

Zinc oxide nanostructures with various benefits such as: cost-effectiveness, non-toxicity, environmentally friendly and large surface area have been widely used as an efficient nanocatalyst in various organic transformations including the Mannich reaction,[21] the Knoevenagel condensation reaction,[22] and the synthesis of 4H-pyrans,[23] β-phosphono malonates,[24] benzimidazole,[25] -acetamido ketones/esters,[26] naphtha[1,2-e] oxazinone,[27] polyhydroquinoline,[28]dihydropyrano[2,3-c] chromenes,[29] 14-aryl-14*H*-dibenzo[a,j]xanthenes.[30]

Herein, in order to achieve a more efficient synthetic process, minimize by-products, decrease the number of separate reaction steps, improving the yields and reaction times and also in extending our research on the application of nanocatalysts in MCRs,[31–36] we wish to report a clean and environmentally friendly approach to the synthesis of tetrahydrobenzo[*a*]xanthen-11-ones *via* multi-component reaction of aldehydes, 2-naphthol and diemdone in the presence of zinc oxide nanoparticles.

2. Results and Discussion

In the preliminary experiments ZnO nanoparticles were prepared and characterized by EDX, XRD, BET, SEM, TEM and IR analysis.

The chemical purity of the samples as well as their stoichiometry was tested by EDX studies. The EDX spectrum given in Fig. 1A shows the presence of zinc and oxygen as the only elementary components.

The crystalline nature of the synthesized ZnO nanoparticles sample was further verified by the X-ray diffraction pattern (XRD). The XRD pattern of the ZnO nanoparticles is shown in

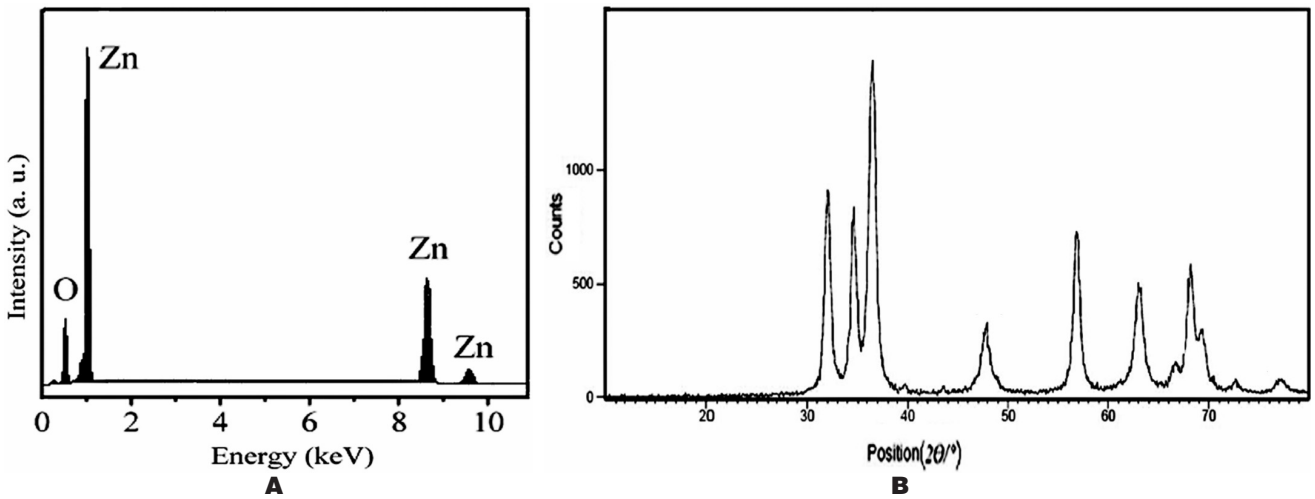

Figure 1 EDX (**A**) and XRD (**B**) of ZnO nanoparticles.

Fig. 1B. All reflection peaks in Fig. 1B can be easily indexed to pure spherical phase of ZnO with P63mc group (JCDPS No. 36-1451). The crystallite size diameter (D) of the ZnO nanoparticles has been calculated by Debye-Scherrer equation ($D = K\lambda/\beta\cos\theta$), where β FWHM (full-width at half-maximum or half-width) is in radian and θ is the position of the maximum of diffraction peak, K is the so-called shape factor, which usually takes a value of about 0.9, and λ is the X-ray wavelength (1.5406 Å for Cu Kα). Crystallite size of ZnO has been found to be 10 nm.

In addition the specific surface area was measured by nitrogen physisorption (the BET method), the specific surface area was approximately 88 $m^2\ g^{-1}$. Also the theoretical particle size was calculated from the surface area and zinc oxide density (6.11 g cm^{-3}) from the equation was 10.6 nm.

$$D_{BET} = \left(\frac{6{,}000}{\rho \times S}\right).$$

Characterization of ZnO NPs structure was continued by SEM and TEM analysis. The SEM image of ZnO nanoparticles is depicted in Fig. 2A. These results show that zinc oxide nanoparticles were obtained from anhydrous $ZnCl_2$ and NaOH with particle size between 10–30 nm under ultrasound power.

The size and morphology of zinc oxide nanoparticles were analyzed by transmission electron microscopy (TEM) (Fig. 2B). The result shows that the smallest sizes of nanoparticles are obtained with a crystalline size about 10 nm, confirming the results calculated from Scherrer's formula based on the XRD pattern.

To study the size distribution of zinc oxide nanoparticles, a particle size distribution histogram was shown in Fig. 3. The results show that most of the particles have a size in the range between 10 and 90 nm. However the smallest particles size obtained is about 10 nm, which confirms the results calculated based on the XRD pattern.

In FT-IR spectrum of ZnO NPs (Fig. 4) the band from 500–600 cm^{-1} is assigned to the stretching vibrations of (Zn–O) bond. The broad band with low intensity at 3422 cm^{-1} is related to vibration mode of (OH) group, indicating the presence of little amount of water adsorbed on the zinc oxide nanoparticles surfaces.

In continuation of this research, in order to explore and optimize various reaction conditions, we selected a multi-component reaction of 4-chlorobenzaldehyde, 2-naphthol and dimedone as a model reaction (Scheme 1).

Initially to evaluate the merit of this method, we carried out the model study in the presence of different catalysts such as MgO, SiO_2, Al_2O_3, TiO_2, CuO, ZnO and ZnO NPs for the synthesis of 12-aryl-8,9,10,12-tetrahydrobenzo[*a*]xanthen-11-ones under

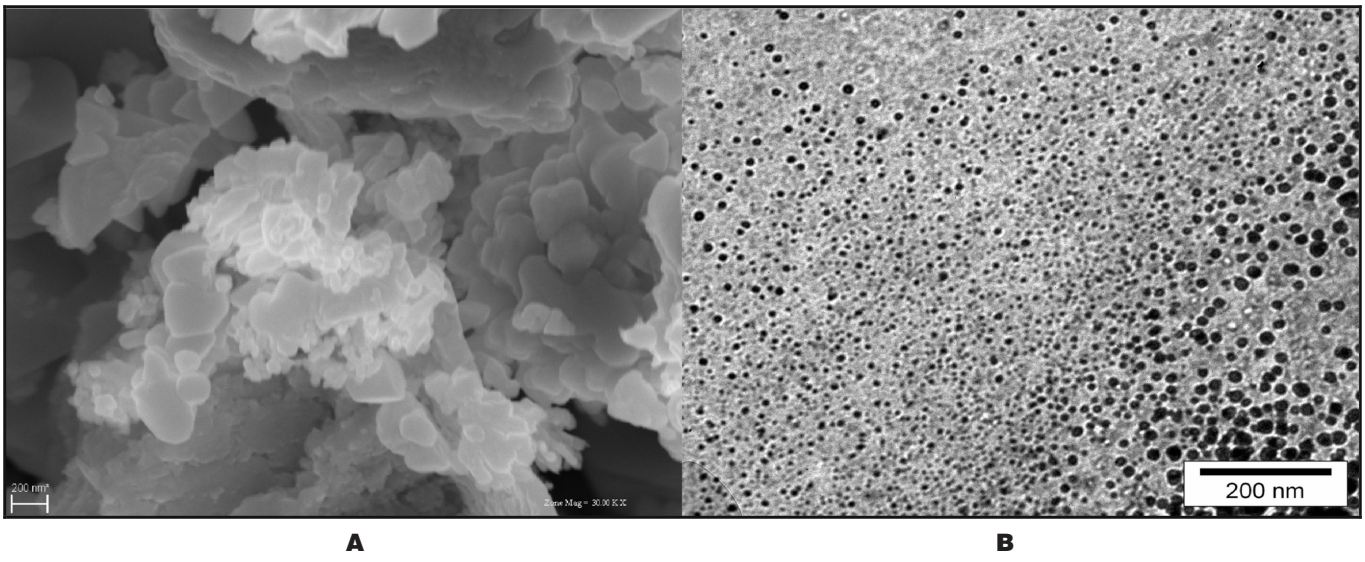

Figure 2 SEM (**A**) and TEM (**B**) of ZnO nanoparticles.

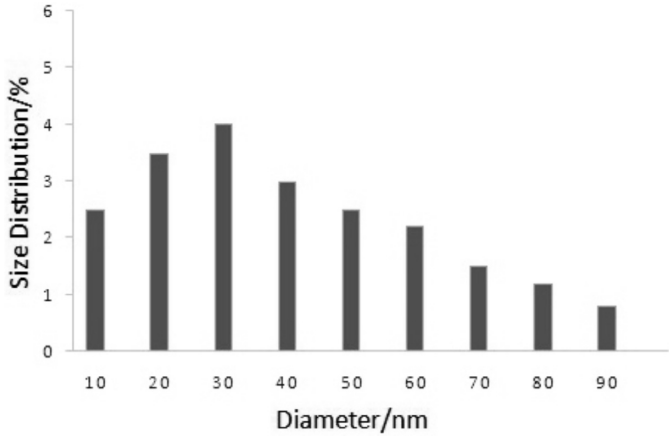

Figure 3 Particle size histogram of ZnO NPs.

solvent-free conditions. As shown in Table 1, zinc oxide nanoparticles were the best catalyst according to reaction times and yield of tetrahydrobenzo[*a*]xanthen-11-one **4d**.

The high catalytic activity of ZnO in comparison to other catalysts may be related to higher surface area available for greater adsorption of the reactants on its surface. So, we were encouraged to use ZnO NPs in the following optimization of the reaction conditions.

In order to optimize the amounts of the zinc oxide nanoparticles, we performed the model reaction using various amounts of the nano ZnO, separately. As indicated in Fig. 5 when increasing the amounts of catalyst from 5 mol% to 10 mol% we have observed better yields for product formation. However, further increase of the molar amount of the catalyst from 10 mol% to 15 mol% did not significantly increase the yield of the product (Fig. 5). Therefore, the optimized amount of ZnO NPs was chosen 10 mol% in the model study.

We have investigated the influence of various solvents and also solvent-free conditions on the three-component coupling of 4-chlorobenzaldehyde, 2-naphthol and dimedone using 10 mol% of zinc oxide nanoparticles. As can be seen from Table 2,

Table 1 The model study for the synthesis of xanthene **4d** by various catalysts.[a]

Entry	Catalyst	Time/min	Yields[b]/%
1	MgO	120	25
2	SiO_2	50	60
3	Al_2O_3	45	55
4	TiO_2	90	44
5	CuO	70	50
6	ZnO	30	65
7	ZnO NPs	12	93

[a] Reaction conditions: molar ratio of aldehyde, 2-naphthol and dimedone (1:1:1); Temperature: 120 °C.
[b] Isolated yield.

it was concluded that solvent-free conditions at 120 °C was the best choice for the preparation of tetrahydrobenzo[*a*] xanthen-11-one **4d.**

Afterwards, the effect of temperature on the rate of reaction was studied by performing the model study under solvent-free conditions. The summarized results of Table 2 show that the best yields and reaction times were obtained at 120 °C.

In this research, we have continued to use zinc oxide nanoparticles in the synthesis a variety of 12-aryl-8,9,10,12-tetrahydrobenzo[*a*]xanthen-11-one derivatives (Scheme 2). We carried out the reaction of 2-naphthol and dimedone with various substituent aryl aldehydes under optimized conditions (solvent-free conditions at 120 °C in the presence of ZnO NPs.

As shown in Table 3 aromatic aldehydes bearing both electron-donating and electron-withdrawing groups can successfully produce a series of tetrahydrobenzo[*a*]xanthen-11-ones in high yields and very short reaction times. Nevertheless aryl aldehydes containing electron-withdrawing groups, for example Cl and NO_2 (Table 3, Entries 3, 4), reacted faster than those bearing electron-donating groups such as OMe and OH (Table 3, Entries 12, 14) as expected. Furthermore, *p*-substituted aryl aldehydes reacted smoothly in comparison to hindered aldehydes.

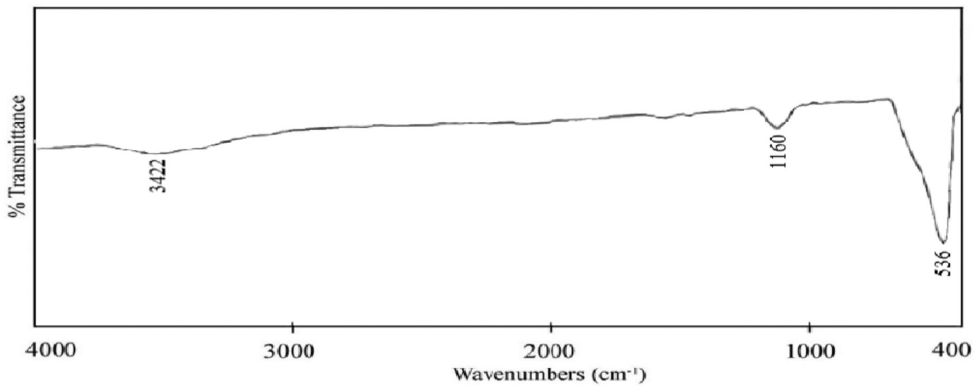

Figure 4 FT-IR spectrum of zinc oxide nanoparticles.

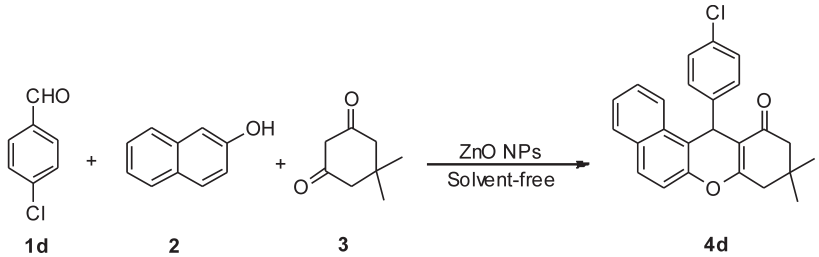

Scheme 1
The model study for the synthesis of racemic tetrahydrobenzo[*a*]xanthen-11-one (**4d**).

Table 2. The model reaction in various solvents catalyzed by ZnO NPs.[a]

Entry	Solvent	T/°C	Time/min	Yields[b]/%
1	EtOH	reflux	120	60
2	DMF	reflux	180	45
3	CH_3CN	reflux	120	55
4	CH_2Cl_2	reflux	240	35
5	$PhCH_3$	reflux	240	trace
6	Solvent-free	r.t.	60	40
7	Solvent-free	50	45	70
8	Solvent-free	100	25	90
9	Solvent-free	120	12	93
10	Solvent-free	140	12	93

[a] Reaction conditions: molar ratio of aldehyde, 2-naphthol and dimedone (1:1:1).
[b] Isolated yields

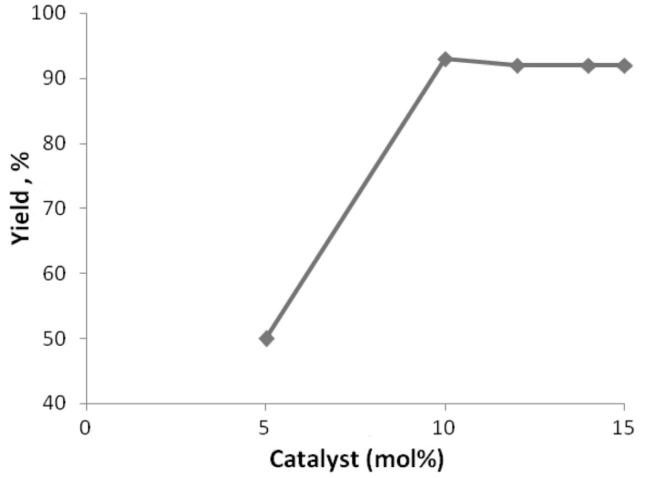

Figure 5 Influence of amount of the ZnO NPs on the model reaction.

In order to determine the catalytic behaviour of ZnO NPs as catalyst for the synthesis of 12-aryl-8,9,10,12-tetrahydrobenzo[*a*]xanthen-11-ones, a plausible reaction mechanism for the reaction of 2-naphthol, aldehydes and dimedone is shown in Scheme 3. We propose that zinc oxide nanoparticles behave as a Lewis acid and coordinate to the carbonyl groups of dimedone and aldehydes that makes them susceptible to nucleophilic attack of other reactants. Finally product 4 was obtained and ZnO NPs nanoparticles being released for further reactions.

3. Experimental

Chemicals were purchased from the Sigma-Aldrich and Merck in high purity. All of the materials were of commercial reagent grade and were used without further purification. Zinc oxide nanoparticles were prepared according to the procedure reported by Rao *et al.*[37] All melting points are uncorrected and

Table 3. Synthesis of 12-aryl-8,9,10,12-tetrahydrobenzo[*a*]xanthen-11-ones using ZnO NPs. Four novel compounds are included.

Entry	Aldehyde (R)	Products	Time/min// Yield [a]/%	M.p./°C [ref]
1	C_6H_5	**4a**	16//88	151–153[10]
2	3-$NO_2C_6H_4$	**4b**	15//90	170–172[10]
3	4-$NO_2C_6H_4$	**4c**	10//95	185–187[10]
4	4-ClC_6H_4	**4d**	12//93	181–182[10]
5	2,4-$Cl_2C_6H_4$	**4e**	20//92	179–181[10]
6	4-BrC_6H_4	**4f**	15//90	181–183[11]
7	4-FC_6H_4	**4g**	15//92	184–185[11]
8	4-CNC_6H_4	**4h**	15//90	168–169 [b]
9	4-$CHOC_6H_4$	**4i**	18//91	192–194 [b]
10	2-$SMeC_6H_4$	**4j**	22//87	203–205 [b]
11	4-$iprC_6H_4$	**4k**	20//86	213–214 [b]
12	4-$OMeC_6H_4$	**4l**	22//88	203–205[10]
13	2-$OMeC_6H_4$	**4m**	30//85	166–168[10]
14	4-OHC_6H_4	**4n**	25//90	212–213[10]
15	3-MeC_6H_4	**4o**	22//85	176–177[13]
16	4-MeC_6H_4	**4p**	18//90	175–177[11]

[a] Isolated yield.
[b] New products.

were determined in capillary tubes with a Boetius melting point microscope. ^{1}H NMR and ^{13}C NMR spectra were obtained on a Bruker 400 MHz spectrometer with $CDCl_3$ as solvent using tetramethylsilane (TMS) as an internal standard, the chemical shift values are in δ (ppm). FT-IR spectra were recorded on a Magna-IR, spectrometer 550 Nicolet in KBr pellets in the range of 400–4000 cm^{-1}. Mass spectra were recorded on a Finnigan MAT 44S by Electron Ionization (EI) mode with an ionization voltage of 70 Ev. The elemental analyses (C, H, N) were obtained from a Carlo ERBA Model EA 1108 analyzer. The N_2 adsorption/desorption analysis (BET) was performed at –196 °C using an automated gas adsorption analyzer (Tristar 3000, Micromeritics). Powder X-ray diffraction (XRD) was carried out on a Philips diffractometer of X'pert Company with mono chromatized Cu Kα radiation (λ = 1.5406 Å). Microscopic morphology of product was visualized by scanning electron microscope (SEM) (LEO 1455VP). The compositional analysis was done by energy dispersive analysis of X-ray (EDX, Kevex, Delta Class I). Transmission electron microscopy (TEM) was performed with a Jeol JEM-2100UHR, operated at 200 kV.

3.1. General Procedure for the Preparation of Zinc Oxide Nanoparticles

To a solution of anhydrous $ZnCl_2$ in deionized water was added NaOH to maintain a PH of 12. Then, the mixture was ultrasonically irradiated for 30 min. The white as-synthesized precipitate was separated by centrifugation and washed with deionized water to remove impurities for several times and then

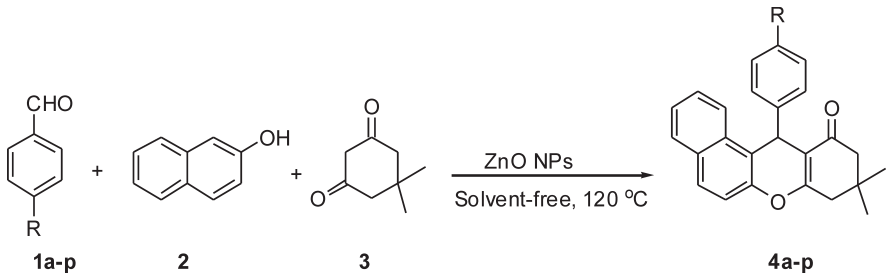

Scheme 2
One-pot synthesis of racemic tetrahydrobenzo[*a*]xanthen-11-ones by zinc oxide nanoparticles.

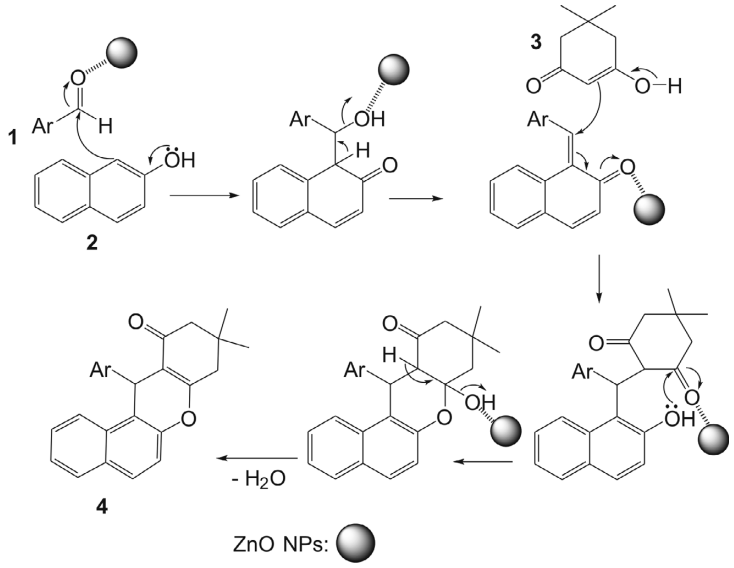

Scheme 3
Proposed reaction pathway for the ZnO nanoparticles catalysis.

dried at 120 °C for 24 h. Finally, the formed nanoparticles were calcined at 600 °C for 12 h to obtain a fine white powder.

3.2. General Procedure for the Synthesis of 12-Aryl-8,9,10,12-tetrahydrobenzo[*a*]xanthen-11-ones (4a–p)

A mixture of aldehyde (1 mmol), 2-naphthol (1 mmol), dimedone (1 mmol) and ZnO NPs (0.007 g, 0.1 mmol, 10 mol%) was finely grinded and heated with stirring at 120 °C in an oil bath. The reaction mixture was monitored by TLC analysis using hexane/ethyl acetate (8:2) and spots were examined using a UV lamp. After cooling, the reaction mixture was dissolved in dichloromethane and the mixture stirred for 5 min. The suspended solution was filtered and then heterogeneous nanocatalyst was recovered. The ethyl acetate was evaporated and the crude product was crystallized from ethanol to afford the pure product.

3.3. Spectral Data of New Products

*4-(9,9-Dimethyl-11-oxo-9,10,11,12-tetrahydro-8*H*-benzo[*a*]xanthen-12-yl)benzonitrile* (**4h**). White crystal; m.p. = 168–169 °C; Rf value 0.60 (hexane/ethyl acetate, 8:2; IR (KBr)/ ν(cm^{-1}): 3066, 2941, 2221 (C≡N), 1648, 1582 (C=C, Ar), 1521(C=C, Ar), 1233 (C-O), ^{1}H NMR ($CDCl_3$)/ δ ppm: d 1.01 (s, 3H, CH_3), 1.15 (s, 3H, CH_3), 2.22–2.35 (m, 2H, CH_2), 2.61–2.62 (m, 2H, CH_2), 5.95 (s, 1H, CH), 7.03–7.05 (d, J = 8.4 Hz, 2H, Ar-H), 7.28–7.30 (m, 2H, Ar-H), 7.39–7.42 (t, J = 7.6 Hz, 1H, Ar-H), 7.48–7.52 (t, J = 7.6 Hz, 1H, Ar-H), 7.76–7.80 (t, 2H, Ar-H), 8.12–8.14 (d, J = 8.4 Hz, 2H, Ar-H); ^{13}C NMR ($CDCl_3$)/ δ ppm: 26.8, 29.1, 32.5, 35.2, 40.9, 51.6, 111.8, 115.8, 117.4, 118.6, 122.9, 123.5, 125.0, 127.4, 128.9, 129.0, 129.6, 130.9, 132.1, 145.8, 147.5, 151.3, 163.9, 196.2; MS (EI) (*m*/*z*): 379 (M^+); (Found: C, 87.30; H, 5.58; N, 3.69 %. Calc. for $C_{26}H_{21}NO_2$ (379.45); C, 87.18; H, 5.69; N, 3.81 %).

*4-(9,9-Dimethyl-11-oxo-9,10,11,12-tetrahydro-8*H*-benzo[*a*]xanthen-12-yl)benzaldehyde* (**4i**). White crystal; m.p. = 192–194 °C; Rf value 0.55 (hexane/ethyl acetate, 8:2; FT-IR (KBr, cm^{-1}): 3052, 2865 (CH, CHO), 1644 (C=C, Ar), 1591, 1236 (C-O). ^{1}H NMR ($CDCl_3$): δ 1.01–1.07 (m, 6H, 2 × CH_3), 2.15–2.25 (m, 2H, CH_2), 2.41–2.51 (m, 2H, CH_2), 5.57 (s, 1H, CH), 7.09–7.11 (d, J = 7.8 Hz, 2H, Ar-H), 7.28–7.35 (m, 3H, Ar-H), 7.73–7.75 (d, J = 7.8 Hz, 2H, Ar-H), 7.80–7.87 (m, 3H, Ar-H), 9.58 (s, 1H); ^{13}C NMR ($CDCl_3$): 27.1, 28.8, 31.3, 36.0, 48.8, 50.5, 111.9, 115.1, 119.9, 121.1, 124.2, 126.5, 127.3, 130.6, 132.6, 134.1, 136.5, 138.0, 145.5, 147.9, 152.1, 164.2, 196.6, 202.9; MS (EI) (m/z): 382 (M^+); (Found: C, 81.65; H, 5.80 %. Calc. for $C_{26}H_{22}O_3$ (382.45); C, 81.73; H, 5.68 %).

*9,9-Dimethyl-12-(4-(methylthio)phenyl)-9,10-dihydro-8*H*-benzo[*a*]xanthen-11(12*H*)-one* (**4j**). White crystal; m.p. = 203–205 °C; Rf value 0.65 (hexane/ethyl acetate, 8:2; FT-IR (KBr, cm^{-1}): 3052, 1636 (C=C, Ar), 1588, 1521 (C=C, Ar), 1222 (C-O), 1191 (C-S). ^{1}H NMR ($CDCl_3$): δ 0.98 (s, 3H, CH_3), 1.13 (s, 3H, CH_3), 2.23–2.34 (m, 2H, CH_2), 2.38 (s, 3H, CH_3), 2.57 (s, 2H, CH_2), 5.67 (s, 1H, CH), 7.05–7.07 (d, J = 8.0 Hz, 2H, Ar-H), 7.25–7.27 (d, J = 8.0 Hz, 2H, Ar-H), 7.31–7.33 (d, J = 8.8 Hz, 1H, Ar-H), 7.37–7.46 (m, 2H, Ar-H), 7.76–7.80 (t, 2H, Ar-H), 7.95–7.97 (d, J = 8.8 Hz, 1H, Ar-H); ^{13}C NMR ($CDCl_3$): 23.8, 27.3, 28.8, 31.3, 35.2, 41.2, 52.7, 110.5, 112.1, 115.2, 116.6, 120.0, 122.4, 124.4, 126.1, 128.2, 130.7, 131.1, 134.8, 143.9, 146.7, 150.1, 160.6, 196.9; MS (EI) (*m*/*z*): 400 (M^+); (Found: C, 77.97; H, 6.04 %. Calc. for $C_{26}H_{24}O_2S$ (400.53); C, 77.82; H, 6.14 %).

*12-(4-Isopropylphenyl)-9,9-dimethyl-9,10-dihydro-8*H*-benzo[*a*]xanthen-11(12*H*)-one* (**4k**). White crystal; m.p.= 213–214 °C; Rf value 0.50 (hexane/ethyl acetate, 8:2; FT-IR (KBr, cm^{-1}): 3041, 1623 (C=C, Ar), 1586, 1511 (C=C, Ar), 1225 (C-O). ^{1}H NMR ($CDCl_3$): δ 0.99 (s, 3H, CH_3), 1.12–1.14 (d, 9H, 3 × CH_3), 2.28–2.29 (m, 2H, CH_2), 2.58 (m, 2H, CH_2), 2.76 (m, 1H, CH), 5.68 (s, 1H, CH), 7.00–7.02 (d, J = 8.0 Hz, 2H, Ar-H), 7.23–7.25 (d, J = 8.0 Hz, 2H, Ar-H), 7.31–7.33 (d, J = 8.8 Hz, 1H, Ar-H), 7.38–7.45 (m, 2H, Ar-H), 7.74–7.79 (t, 2H, Ar-H), 8.03–8.05 (d, J = 8.8 Hz, 1H, Ar-H); ^{13}C NMR ($CDCl_3$):): 23.3, 23.6, 26.9, 29.2, 32.1, 34.6, 35.8, 40.1, 52.7, 111.1, 113.2, 114.8, 114.9, 118.1, 120.5, 123.1, 125.9, 127.1, 128.7, 130.2, 133.1, 138.1, 142.8, 154.3, 163.9, 196.4; MS (EI) (*m*/*z*): 396 (M^+); (Found: C, 84.81; H, 7.12 %. Calc. for $C_{28}H_{28}O_2$ (396.52); C, 84.96; H, 7.02 %).

3.3. Recycling and Reusing of the Catalyst

After completion of the reaction, the catalyst was washed well using dichloromethane and ethyl acetate and then dried at 100 °C for 8 h. The reusability of ZnO NPs was tested by repeat-

Table 4 Recoverability of the ZnO nanoparticles.

Yield/%				
First	Second	Third	Fourth	Fifth
97	96	95	93	88

ing the model study in the presence of zinc oxide nanoparticles under optimized conditions. The results of these experiments showed that the catalytic activity of the nanocatalyst did not decrease significantly even after five catalytic cycles (Table 4).

4. Conclusion

In this research, we have successfully demonstrated unique catalytic activity of zinc oxide nanoparticles in the synthesis of 12-aryl-8,9,10,12-tetrahydrobenzo[*a*]xanthen-1-ones *via* multi-component reactions of aldehydes, 2-naphthol and dimedone under solvent-free conditions. A total of four novel compounds were also reported. The present approach is easy, efficient and eco-friendly and the products were obtained in excellent yields and short reaction times. Also zinc oxide nanoparticles have significant advantages such as being economical, and because of their recoverability, reusability and stability.

Acknowledgements

The authors gratefully acknowledge the financial support of this work by the Research Affairs Office of the Islamic Azad University, Qom Branch, Qom, Iran.

References

1 M. Syamala, *Org. Prep. Proced. Int.,* 2009, **41**, 1–68.
2 G. Evano, N. Blanchard and M. Toumi, *Chem. Rev.*, 2008, **108**, 3054–3133.
3 (a) H.N. Hafez, M.I. Hegab, I.S. Ahmed-Farag and A.B.A. El-Gazzar, *Bioorg. Med. Chem. Lett.,* 2008, **18**, 4538–4543. (b) M.M.M. Pinto, M.E. Sousa and M.S.J. Nascimento, *Curr. Med. Chem.*, 2005, **12**, 2517–2538.
4 (a) R.W. Lambert, J.A. Martin, J.H. Merrett, K.E.B. Parkes and G.J. Thomas, PCT Int. Appl. WO9706178, 1997; *Chem. Abstr.* 1997, 126, p212377y. (b) G.J. Bennett and H.-H. Lee, *Phytochem.*, 1989, **28**, 967–998.
5 (a) T. Hideo and J. Teruomi, Jpn. Tokkyo Koho JP56005480, 1981; *Chem. Abstr.* 1981, 95, 80922b. (b) V. Peres, T.J. Nagem and F.F. de Oliveira, *Phytochem.*, 2000, **55**, 683–710.
6 R.-M. Ion, *Prog. Catal.*, 1997, **6**, 55–76.
7 C.G. Knight and T. Stephens, *Biochem. J.,* 1989, **258**, 683–687.
8 S.M. Menchen, S.C. Benson, J.Y.L. Lam, W. Zhen, D. Sun, B.B. Rosenblum, S.H. Khan and M. Taing, U.S. Patent, US 6583168, 2003; *Chem. Abstr.* 2003, 139. p54287f.
9 M. Ahmad, T.A. King, K. Do-Kyeong, B.H. Cha and L. Jongmin, *J. Phys. D: Appl. Phys.,* 2002, **35**, 1473–1476.
10 Z. Hongjun, Z. Yong, C. Bowen, Z. Weiwei, X. Xianlin and R. Yuanlin, *Chin. J. Chem.*, 2012, **30**, 362–366.
11 J.M. Khurana, A. Lumb, A. Pandey and D. Magoo, *Synth. Commun.*, 2012, **42**, 1796–1803.
12 G.C. Nandi, S. Samai, R. Kumar and M.S. Singh, *Tetrahedron*, 2009, **65**, 7129–7134.
13 A. Zare, R. Khanivar, M. Hatami, M. Mokhlesi, M.A. Zolfigol, A.R. Moosavi-Zare, A. Hasaninejad, A. Khazaei and V. Khakyzadeh, *J. Mex. Chem. Soc.*, 2012, **56**, 389–394.
14 Z.-H. Zhang, P. Zhang, S.-H. Yang, H.-J. Wang and J. Deng, *J. Chem. Sci.*, 2010, **122**, 427–432.
15 R.-Z. Wang, L.-F. Zhang and Z.-S. Cui, *Synth. Commun.*, 2009, **39**, 2101–2107.
16 P.V. Shinde, A.H. Kategaonkar, B.B. Shingate and M.S. Shingare, *Beilstein J. Org. Chem.*, 2011, **7**, 53–58.
17 D. Fang, J.-M. Yang and Y.-F. Cao, *Res. Chem. Intermed.*, 2013, **39**, 1745–1751.
18 L.-P. Mo and H.-L. Chen, *J. Chin. Chem. Soc.*, 2010, **57**, 157–161.
19 G.S. McCarty and P.S. Weiss, *Chem. Rev.,* 1999, **99**, 1983–1990.
20 A. A. Yelwande, M.E. Navgire, D.T. Tayde, B.R. Arbad and M.K. Lande, *S. Afr. J. Chem.*, 2012, **65**, 131–137.
21 D. I. MaGee, M. Dabiri, P. Salehi and L. Torkian, *Arkivoc*, 2011, **11**, 156–164.
22 M. Sarvari, H, Sharghi and S. Etemad, *Helv. Chim. Acta.,* 2008, **91**, 715–724.
23 P. Bhattacharyya, K. Pradhan, S. Paul and A.R. Das, *Tetrahedron Lett.*, 2012, **53**, 4687–4691.
24 M. Sarvari and S. Etemad, *Tetrahedron*, 2008, **64**, 5519–5523.
25 H. Alinezhad, F. Salehian and P. Biparva, *Synth. Commun.*, 2012, **42**, 102–108.
26 Z. Mirjafary, H. Saeidian, A. Sadeghi and F.M. Moghaddam, *Catal. Commun.*, 2008, **9**, 299–306.
27 G.B.D. Rao, M.P. Kaushik and A.K. Halve, *Tetrahedron Lett.*, 2012**, 53**, 2741–2744.
28 M.Z. Kassaee, H. Masrouri and F. Movahedi, *Monatsh. Chem.*, 201**0, 141**, 317–332.
29 S. Paul, P. Bhattacharyya and A.R. Das, *Tetrahedron Lett.,* 2011**, 52**, 4636–464.
30 J. Safaei-Ghomi and M.A. Ghasemzadeh, *Chin. Chem. Lett.,* 2012, **23**, 1225–1229.
31 J. Safaei-Ghomi and M.A. Ghasemzadeh, *J. Sulfur. Chem.,* 2013, **34**, 233–241.
32 M.A. Ghasemzadeh, J. Safaei-Ghomi and H. Molaei, *C. R. Chimie.*, 2012, **15**, 969–974.
33 J. Safaei-Ghomi, M.A. Ghasemzadeh and M. Mehrabi, *Sci. Iran. Trans. C.*, 2013, **20**, 549–554.
34 M.A. Ghasemzadeh, J. Safaei-Ghomi and S. Zahedi, *J. Serb. Chem. Soc.,* 2013, 78, 769–779.
35 J. Safaei-Ghomi, M.A. Ghasemzadeh and S. Zahedi, *S. Afr. J. Chem.*, 2012, **65**, 191–195.
36 J. Safaei-Ghomi, M.A. Ghasemzadeh and A. Kakavand-Qalenoei, *J. Saud. Chem. Soc.*, in press: http://dx.doi.org/10.1016/j.jscs.2012.07.010.
37 G.B.D. Rao, M.P. Kaushik and A.K. Halve, *Tetrahedron Lett.*, 2012, **53**, 2741–2744.